Molecular Therapy
Nucleic Acids
Original Article

The miR-148/152 family contributes to angiogenesis of human pluripotent stem cell-derived endothelial cells by inhibiting MEOX2

Fengyue Ding,[1,2] Hongchun Wu,[1,2] Xinglong Han,[1,2] Xue Jiang,[1] Yang Xiao,[1] Yuanyuan Tu,[1] Miao Yu,[1] Wei Lei,[1] and Shijun Hu[1]

[1]Department of Cardiovascular Surgery of the First Affiliated Hospital & Institute for Cardiovascular Science, Collaborative Innovation Center of Hematology, State Key Laboratory of Radiation Medicine and Protection, Suzhou Medical College, Soochow University, Suzhou 215000, China

Human pluripotent stem cell-derived endothelial cells (hPSC-ECs) represent a promising source of human ECs urgently needed for the study of cardiovascular disease mechanisms, cell therapy, and drug screening. This study aims to explore the function and regulatory mechanism of the miR-148/152 family consisting of miR-148a, miR-148b, and miR-152 in hPSC-ECs, so as to provide new targets for improving EC function during the above applications. In comparison with the wild-type (WT) group, miR-148/152 family knockout (TKO) significantly reduced the endothelial differentiation efficiency of human embryonic stem cells (hESCs), and impaired the proliferation, migration, and capillary-like tube formatting abilities of their derived ECs (hESC-ECs). Overexpression of miR-152 partially restored the angiogenic capacity of TKO hESC-ECs. Furthermore, the mesenchyme homeobox 2 (MEOX2) was validated as the direct target of miR-148/152 family. MEOX2 knockdown resulted in partial restoration of the angiogenesis ability of TKO hESC-ECs. The Matrigel plug assay further revealed that the *in vivo* angiogenic capacity of hESC-ECs was impaired by miR-148/152 family knockout, and increased by miR-152 overexpression. Thus, the miR-148/152 family is crucial for maintaining the angiogenesis ability of hPSC-ECs, and might be used as a target to enhance the functional benefit of EC therapy and promote endogenous revascularization.

INTRODUCTION

Endothelial cells (ECs) that line the blood and lymphatic vessels regulate many critical physiological processes including metabolic homeostasis, vascular hemodynamics, vascular permeability, coagulation, and cell extravasation.[1,2] Endothelial dysfunction is regarded as not only one of the leading causes and hallmarks of vascular pathologies such as hypertension, coronary artery disease, and diabetes mellitus, but also a contributor of nonvascular diseases including neurodegeneration and chronic inflammatory disorders.[3] Human pluripotent stem cells (hPSCs), including human induced pluripotent stem cells (hiPSCs) and human embryonic stem cells (hESCs), have emerged as a promising source of human ECs for cell therapy, drug screening, tissue engineering, or mechanism investigation of endothelial dysfunction in certain diseases.[4,5] Studies have reported that transplantation of hPSC-derived ECs (hPSC-ECs) into the hearts or other ischemic sites can facilitate therapeutic vascular regeneration and improve functional recovery after ischemic injury.[6–9] Even so, the applications of hPSC-ECs have fallen behind those of parenchymal cell types in the injury tissues. Better understanding and control of various cellular and molecular aspects of angiogenesis, using hPSC-ECs as a surrogate human vascular model, will profoundly enhance our ability to treat diseases with ischemic and endothelial dysfunction components.

MicroRNAs (miRNAs) are a class of small non-coding RNAs (~22 nucleotides) that regulate specific target mRNAs through a complementary match to cleave mRNAs or inhibit protein translation.[10,11] Accumulating studies have shown the capacity of endothelial miRNAs to regulate EC differentiation, homeostasis, and angiogenesis.[12–16] For example, miR-99b, miR-191a, and miR-181b are capable of potentiating EC differentiation from hESCs and improving hESC-EC-induced therapeutic neovascularization *in vivo*.[17] Other miRNAs mediating EC lineage specification include miR-21, miR-200c, miR-150, miR-6086/6087, miR-5739, and so on.[18,19] MiR-126, among other miRNAs, was shown to promote angiogenesis and EC function by inhibiting the negative regulators of vascular endothelial growth factor (VEGF) signaling, including the sprouty related EVH1 domain containing 1 (SPRED1) and phosphoinositide-3-kinase regulatory subunit 2 (PIK3R2).[20] The promising pro-angiogenic potential

Received 18 October 2022; accepted 19 April 2023;
https://doi.org/10.1016/j.omtn.2023.04.020.

[2]These authors contributed equally

Correspondence: Wei Lei, Department of Cardiovascular Surgery of the First Affiliated Hospital & Institute for Cardiovascular Science, Collaborative Innovation Center of Hematology, State Key Laboratory of Radiation Medicine and Protection, Suzhou Medical College, Soochow University, Suzhou 215000, China.
E-mail: leiwei@suda.edu.cn
Correspondence: Shijun Hu, Department of Cardiovascular Surgery of the First Affiliated Hospital & Institute for Cardiovascular Science, Collaborative Innovation Center of Hematology, State Key Laboratory of Radiation Medicine and Protection, Suzhou Medical College, Soochow University, Suzhou 215000, China.
E-mail: shijunhu@suda.edu.cn

of these miRNAs will be helpful for generation of optimized ECs for cardiovascular repair therapies.

The microRNA-148/152 (miR-148/152) family consisting of miR-148a, miR-148b, and miR-152, which share the same seed sequences, has been widely involved in tumorigenesis, autoimmune diseases, and ventricular remodeling.[21–23] However, conflicting evidence has been reported concerning the role of miR-148/152 family members in angiogenesis. While all miR-148/152 family members have been shown to inhibit migration of ECs and reduce tumor angiogenesis,[21,24] topical delivery of miR-148b mimics promoted angiogenesis and accelerated wound healing *in vivo*.[25] Further investigations in other models are needed to elucidate the roles and underlying mechanisms of miR-148/152 family members in angiogenesis.

Human PSCs present a promising human cell resource for investigating the functions of genes, due to their potential to differentiate into any human cells and their accessibility to genetic manipulation. We previously generated two hESC lines with triple knockout of miR-148/152 family members, and demonstrated a critical role of the miR-148/152 family in maintaining lateral mesoderm/cardiomyocyte fate from hESCs.[26] In present study, by using these two cell lines, we further investigated the role of the miR-148/152 family in EC differentiation and angiogenesis. Our results indicated that triple knockout of the miR-148/152 family reduced the efficiency of EC differentiation, and inhibited the angiogenic capacity of hESC-ECs, which is partially mediated by the mesenchyme homeobox 2 (MEOX2).

RESULTS

Deletion of the miR-148/152 family inhibits endothelial differentiation from hESCs

The miR-148/152 family is composed of miR-148a, miR-148b, and miR-152, which share almost identical sequence (Figure 1A) and thus are speculated to regulate similar target genes and cellular functions. Our RT-qPCR results demonstrated a significantly increased expression of all the three members in ECs derived from either hESCs or hiPSCs, indicating that the miR-148/152 family may play a certain function in ECs (Figure 1B). We thus attended to assess the role of the miR-148/152 family in EC differentiation and endothelial function via gain/loss-of-function approaches in hESCs and hESC-derived ECs (hESC-ECs). In this study, we used two previously generated miR-148a/148b/152 triple-knockout hESC lines (TKO#1 and TKO#2), which can avoid the functional complementation among three members observed in the single-family member knockout cells.[26] Before EC differentiation, we briefly verified the pluripotency of the TKO cell lines, as shown by comparable expressions of pluripotent markers NANOG and SOX2 in wild-type (WT) and TKO hESCs (Figure S1), as well as the knockout efficiency of miR-148/152 family members in these cells (Figure 1C).

To obtain human ECs, we initiated mesoderm commitment from hESCs via temporally activing Wnt signaling with CHIR, and promoted their further differentiation into ECs by subsequent treatment with basic fibroblast growth factor (bFGF), VEGF, and bone morphogenetic protein 4 (BMP4) (Figure 1D). On day 6 of EC differentiation, we noticed an obvious decrease in the efficiency of EC differentiation from TKO hESCs when compared with that from WT hESCs (Figures 1E and 1F). This is not surprising, since triple knockout of the miR-148/152 family in hESCs has been shown to inhibit the commitment of cardiac mesoderm, the origin of both cardiomyocytes and cardiac ECs.[26] Consistently, the expression of Delta-like 1 (DLL1), a direct target of the miR-148/152 family that suppresses cardiac mesoderm differentiation, was significantly upregulated in TKO hESC-derived cells on day 3 of EC differentiation (Figure 1G).

After $CD34^+$ magnetic-activated cell sorting (MACS) purification on day 6 of EC differentiation, we observed significantly decreased expression of pluripotent markers (SOX2 and OCT3/4) and increased expression of endothelial cell markers (CD31 and CD144) in both WT and TKO hESC-ECs, when compared with that in hESCs (Figure S2). However, their expressions are comparable among WT hESC-ECs and TKO hESC-ECs, as well as the primary human umbilical vein endothelial cells (HUVECs) (Figure S2). Immunofluorescence and DiI-ac-LDL uptake assays showed that deletion of the miR-148/152 family neither disrupted membrane localization of CD31 protein (Figure 1H), nor interfered with uptake of DiI-ac-LDL by hESC-ECs (Figure 1I).

Collectively, these data indicate that triple knockout of the miR-148/152 family impairs the efficiency of hESC differentiation into ECs, but does not alter the endothelial characteristics of hESC-ECs.

Deletion of the miR-148/152 family impairs angiogenic capacity of hESC-ECs

We then attended to assess the angiogenic capacity of WT and TKO hESC-ECs. First, we confirmed the efficient knockout of miR-148/152 family members in $CD34^+$ ECs derived from both TKO hESC lines by RT-qPCR (Figure S3). Whereafter, the major cellular events associated with angiogenesis, including EC proliferation, migration, and vessel formation, were respectively assessed in this study.

As shown in Figure 2A, despite the same initial cell number and split ratio, TKO (TKO#1 and TKO#2) hESC-ECs at passage 4 showed much lower densities than WT hESC-ECs. These data were further confirmed by cell counting assay (Figure 2B). In addition, flow cytometry-based EdU assay revealed that the proportion of proliferative cells (EdU^+ cells) was significantly lower in TKO hESC-ECs than WT hESC-ECs (Figures 2C and 2D). These data demonstrated an adverse effect of miR-148/152 knockout on cell proliferation in hESC-ECs.

We then performed a wound-healing assay to investigate the effect of the miR-148/152 family on the migration ability of hESC-ECs. As shown in Figure 1E, wound was introduced in each confluent monolayer of TKO hESC-ECs by mechanically scratching with a pipet tip. The wound area was obviously reduced in both WT and TKO groups in 12 h due to cell migration from the wound edge. However, cell migration at the wound area was significantly decreased in TKO groups

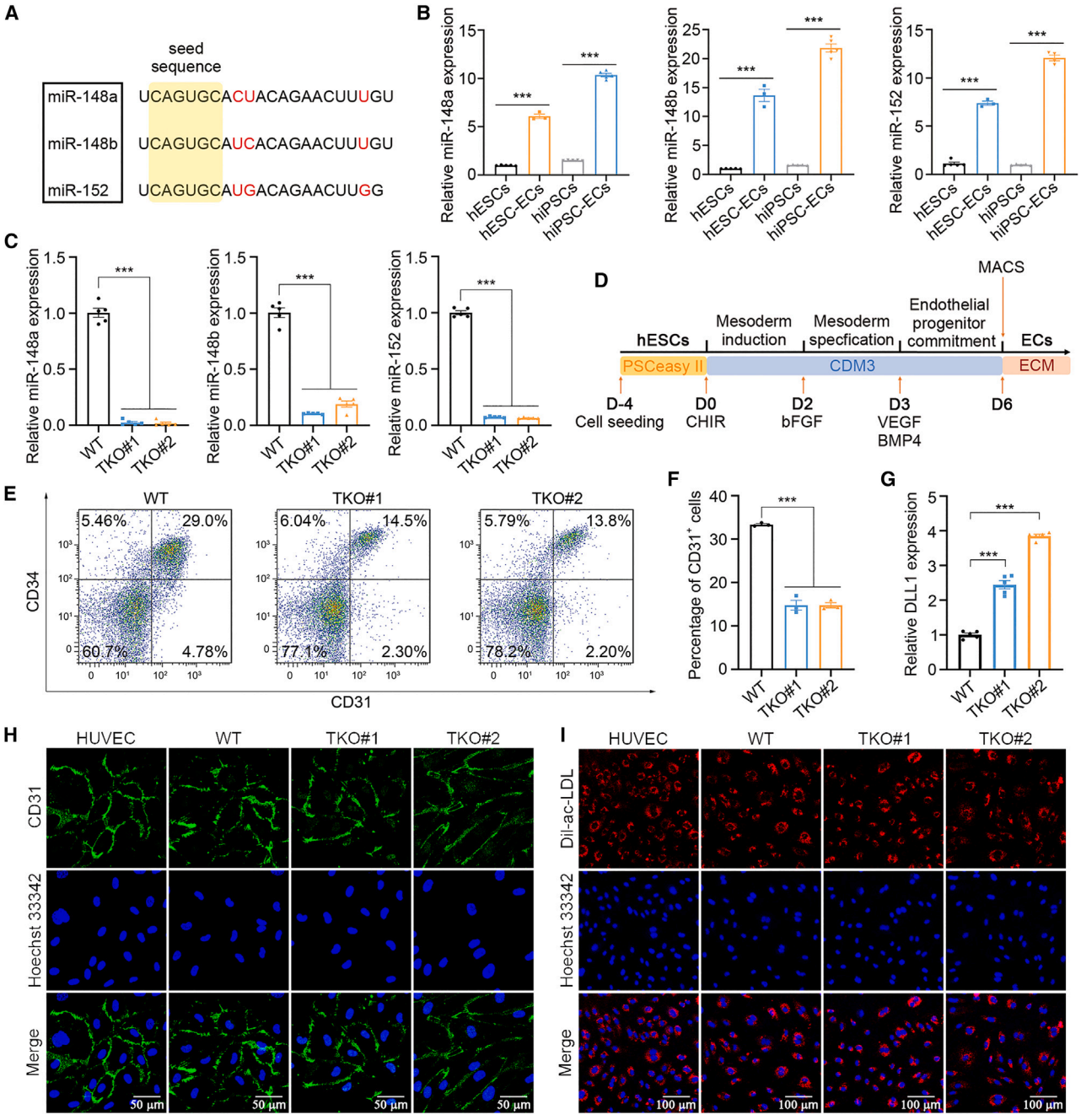

Figure 1. Deletion of the miR-148/152 family inhibits EC differentiation from hESCs

(A) The sequence comparison of the miR-148/152 family members. (B) RT-qPCR detection of the miR-148/152 family in hESCs, hiPSCs, and the differentiated ECs (n = 5 per group). hESCs, human embryonic stem cells; hESC-ECs, hESC-derived endothelial cells; hiPSCs, human induced pluripotent stem cells; hiPSC-ECs, hiPSC-derived endothelial cells. (C) RT-qPCR detection of miR-148/152 family in wild-type (WT) and miR-148/152 family triple-knockout (TKO) hESCs (n = 5 per group). (D) Schematic diagram of EC differentiation from hESCs *in vitro*. (E) Flow cytometry analysis of CD31 and CD34-positive ECs on day 6 of endothelial differentiation from WT and TKO hESCs. (F) Quantitative statistics of CD31-positive cells in (E) (n = 3 per group). (G) RT-qPCR detection of DLL1, a direct target of the miR-148/152 family that inhibits the formation of cardiac mesoderm, in WT and TKO hESC-derived cells on day 3 of endothelial differentiation (n = 5 per group). (H) Immunofluorescence staining of WT and TKO hESC-derived ECs with CD31 (green) and Hoechst 33342 (blue). Scale bar indicates 50 μm. (I) Immunofluorescence detection of the low-density lipoprotein (Dil-ac-LDL, red) uptake by WT and TKO hESC-derived ECs. Nuclei were stained with Hoechst 33342 (blue). Scale bar indicates 100 μm. The statistical data are expressed as the mean ± SEM. ***$p < 0.001$.

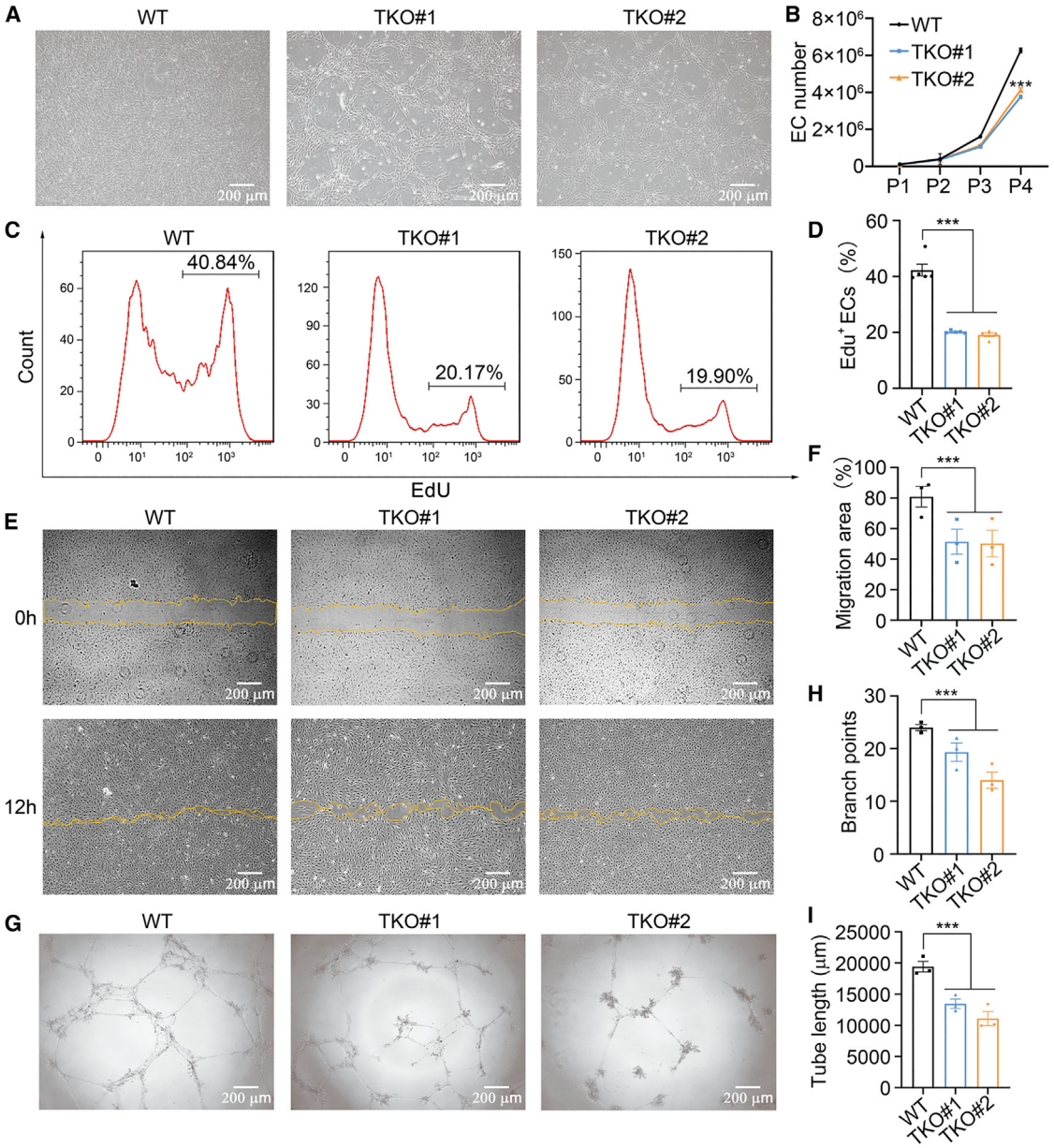

Figure 2. Deletion of miR-148/152 family in ECs inhibits angiogenesis

(A) Representative bright-field images of WT and TKO hESC-derived ECs at passage 4. (B) Total number of ECs at passages 1 to 4 (n = 4 per group). (C) EdU cell proliferation assays in WT and TKO hESC-derived ECs by flow cytometry. (D) Statistical analysis of EdU-positive ECs in EdU cell proliferation assays (n = 5 per group). (E) Representative bright-field images of wound-healing assay performed in WT and TKO hESC-derived ECs. (F) Quantitative statistics of migration area in the wound-healing assays (n = 3 per group). (G) Representative bright-field images of tube formation on Matrigel performed in WT and TKO hESC-derived ECs. (H) Statistical analysis of branch points formed by WT and TKO hESC-derived ECs (n = 3 per group). (I) Statistical analysis of the total length of capillary tubes formed by WT and TKO hESC-derived ECs (n = 3 per group). Scale bar indicates 200 μm. The data are expressed as the mean ± SEM. ***$p < 0.001$.

when compared with that in WT group (Figure 2F), indicating that miR-148/152 knockout is detrimental for EC migration.

Tube formation is a powerful model for studying endothelial angiogenesis *in vitro*. By using tube formation assay, we found that miR-148/152 knockout led to defective formation of capillary-like tubes in hESC-ECs (Figure 2G). The number of branch points and total tube length, as quantified with angiogenesis analyzer plugin for ImageJ, were significantly decreased in both TKO#1 and TKO#2 hESC-ECs when compared with WT hESC-ECs (Figures 2H and 2I).

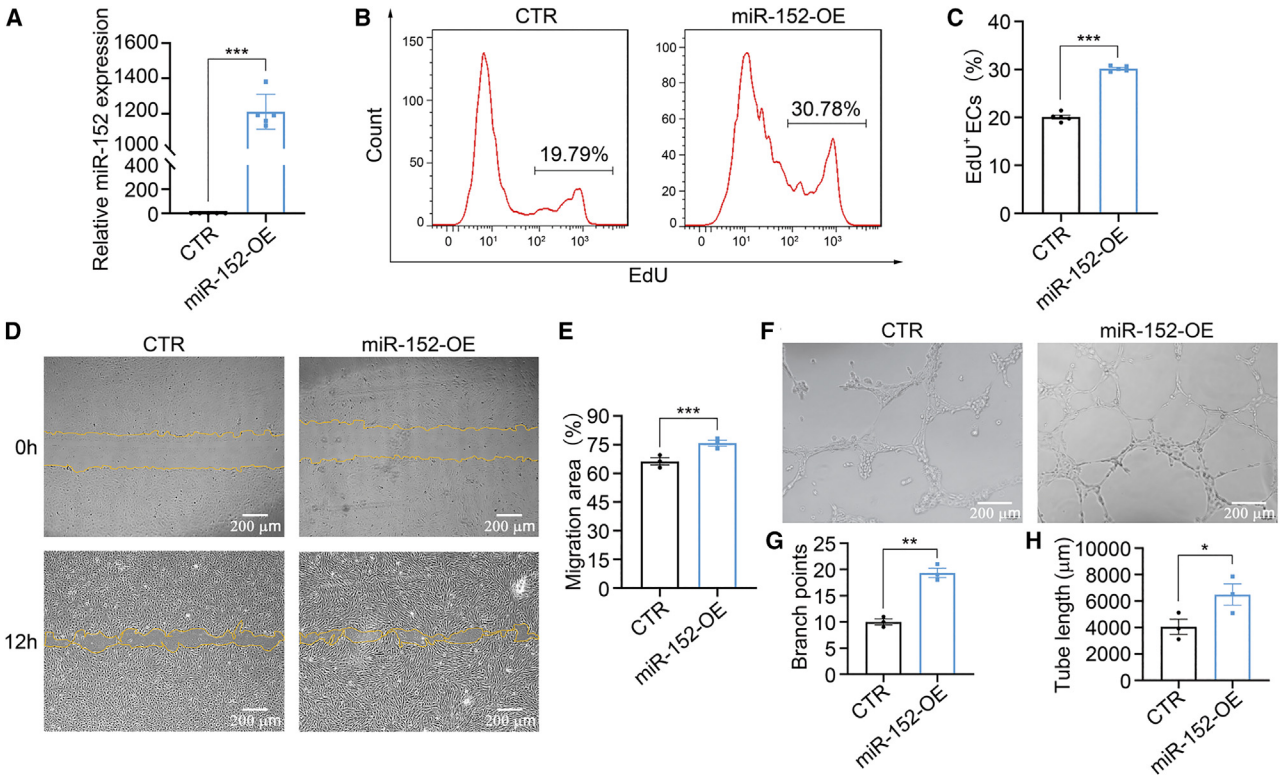

Figure 3. miR-152 overexpression restored the angiogenesis capacity of TKO hESC-derived ECs

(A) Verification of miR-152 overexpression in TKO hESC-derived ECs by RT-qPCR (n = 5 per group). (B) Flow cytometric assay of EdU incorporation into TKO hESC-derived ECs after miR-152 overexpression. (C) Statistical analysis of EdU-positive ECs (n = 5 per group). (D) Representative bright-field images of wound-healing assay performed in TKO hESC-derived ECs with/without miR-152 overexpression. (E) Quantitative statistics of migration area in the wound-healing assays (n = 3 per group). (F) Representative bright-field images of tube formation on Matrigel performed in TKO hESC-derived ECs with/without miR-152 overexpression. (G) Statistical analysis of branch points formed in the tube formation assays (n = 3 per group). (H) Statistical analysis of the total length of capillary tubes formed in the tube formation assays (n = 3 per group). Scale bar indicates 200 μm. The data are expressed as the mean ± SEM. *$p < 0.05$, **$p < 0.01$, ***$p < 0.001$.

Above results indicate that deletion of the miR-148/152 family abrogates angiogenesis in hESC-ECs via impairing cell proliferation, migration, and capillary-like tube formation. We also analyzed cell apoptosis in WT and TKO hESC-ECs by Annexin V-APC/7-AAD-stained flow cytometry, but failed to detect an obvious difference between the two groups, either under normal culture condition or under the conditions of hydrogen peroxide (H_2O_2) treatment (Figure S4).

miR-152 overexpression improves angiogenic capacity of WT and TKO hESC-ECs

To validate the roles of miR-148/152 family deficiency in endothelial dysfunction, we further performed rescue experiments through lentivirus-mediated overexpression of miR-152, as a representative of the miR-148/152 family, in TKO#1 hESC-ECs. Along with successful overexpression of miR-152 (Figure 3A), the proliferation ability of TKO#1 hESC-ECs was obviously restored, as indicated by a significant increase of EdU-positive cells after miR-152 overexpression (Figures 3B and 3C). Meanwhile, miR-152 overexpression in TKO#1 hESC-ECs significantly increased the cell migration area in wound-healing assay (Figures 3D and 3E), and promoted capillary-like tube formation as compared with the control (Figures 3F–3H).

In order to assess the pro-angiogenic effect of miR-152 in other human EC sources, WT hESC-ECs, HUVEC and EA.hy926 cells were transfected with miR-152-overexpressing lentiviral particles, followed by tube formation assay. Our data indicated that miR-152 overexpression could also promote tube network formation of different ECs in a dose-dependent pattern (Figure S5).

Taken together, our data indicate that the miR-148/152 family plays a critical role in maintaining the angiogenic capacity of hESC-ECs and other ECs via promoting EC proliferation, migration, and tube formation.

MEOX2 is a direct target gene of the miR-148/152 family involving cell-cycle arrest

To investigate the mechanism by which the miR-148/152 family regulates angiogenesis, we predicted the potential targets of the miR-148/152 family using the TargetScan online tool. Gene

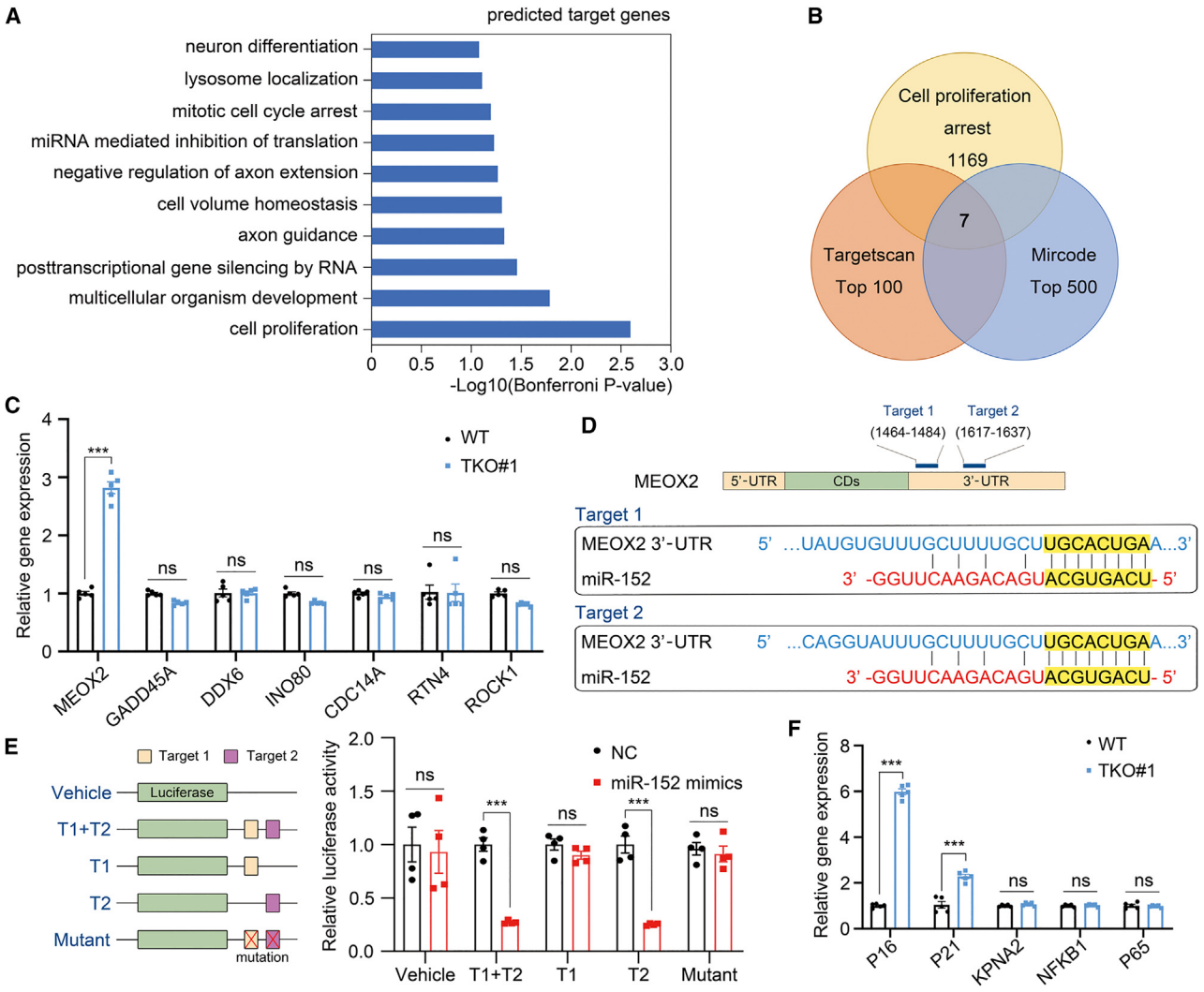

Figure 4. MEOX2 is a direct target gene of the miR-148/152 family

(A) Gene ontology (GO) assay of predicted targets of the miR-148/152 family. (B) Venn diagram showing the overlap of genes between cell proliferation arrest sets and targets of the miR-148/152 family predicted by both TargetScan and Mircode. (C) RT-qPCR detection of the predicted targets of the miR-148/152 family associated with cell arrest in WT and TKO hESC-derived ECs (n = 5 per group). (D) Diagram depicting the sequence alignment of miR-152 and its target sites within the MEOX2 3′-UTR. (E) Schematic diagram of luciferase reporter system for MEOX2 3′-UTR that contains predicated target sites of the miR-148/152 family and luciferase analysis showing an inhibitory effect of miR-152 mimics on the activity of MEOX2 3′-UTR (n = 4 per group). (F) RT-qPCR detection of the downstream genes of MEOX2 including P16, P21, KPNA2, NFKB1, and P65 in WT and TKO hESC-derived ECs (n = 5 per group). The data are expressed as the mean ± SEM. ***p < 0.001, ns indicates not significant.

ontology analysis revealed enrichments of the top 100 TargetScan-predicted targets in many biological processes, including cell proliferation, multicellular organism development, and mitotic cell-cycle arrest that are involved in angiogenesis (Figure 4A). Since the miR-148a/152 family is supposed to inhibit the negative regulators of angiogenesis, we questioned whether cell-cycle arrest-related genes contributed to miR-148/152 family-induced angiogenesis in hESC-ECs. We found seven cell-cycle arrest-related genes among the potential targets of the miR-148/152 family predicted by both TargetScan and Mircode (Figure 4B). However, only MEOX2, which encodes homeobox protein MOX-2, showed significantly increased expression in the TKO hESC-ECs when compared with the WT hESC-ECs (Figure 4C).

Two target sites were predicated in the 3′-UTR of MEOX2 (Figure 4D). Therefore, we performed dual luciferase assay to validate the action of the miR-148/152 family on the 3′-UTR of MEOX2 (Figure 4E). Compared with the miRNA control, miR-152 mimics significantly undermined the luciferase activities of 3′-UTR-reporter constructs carrying both target sites or carrying only the second target site (Figure 4E). However, miR-152 mimics failed to inhibit the luciferase activity of the 3′-UTR-reporter constructs carrying the mutant

target sites (Figure 4E). These data revealed that MEOX2 is indeed a direct target gene of the miR-148/152 family, and negatively regulated by miR-148/152 family. Consistently, two known target genes of MEOX2, including P16 and P21, were dramatically upregulated in TKO hESC-ECs when compared with that in WT hESC-ECs (Figure 4F).

MEOX2 knockdown promotes angiogenesis in TKO hESC-ECs

Since MEOX2 is a direct target of the miR-148/152 family and upregulated by the deletion of the miR-148/152 family, we investigated whether MEOX2 mediates the pro-angiogenesis role of the miR-148/152 family by knocking down MEOX2 expression in TKO hESC-ECs. RT-qPCR data showed that MEOX2 small hairpin RNAs (shRNAs) led to about 60%–70% knockdown of MEOX2 mRNAs in TKO#1 hESC-ECs relative to the non-targeted shRNA group (Figure 5A), along with significant inhibition of its downstream target gene P16, P21, KPNA2, NFKB1, and P65 (Figure 5B). Probably due to sufficient expression of MEOX2 at physiological state or the existence of other gene-mediated regulation, miR-148/152 family knockout led to less affection on these target genes (Figure 4F). After MEOX2 knockdown for 48 h, we assessed the cell proliferation, migration, and tube formation capacities in TKO#1 hESC-ECs. The proportion of EdU^+ cells significantly increased in TKO#1 hESC-ECs subjected to MEOX2 inhibition (Figures 5C and 5D). Meanwhile, MEOX2 knockdown resulted in partial restoration of the migration and tube formation abilities of TKO#1 hESC-ECs (Figures 5E–5I). Taken together, MEOX2 is a direct target gene of the miR-148/152 family and a key mediator of the pro-angiogenesis effect of the miR-148/152 family in hESC-ECs.

The miR-148/152 family is critical for maintaining angiogenic capacity of hESC-ECs *in vivo*

To validate whether miR-148/152 could also regulate the angiogenesis of hESC-ECs *in vivo*, we conducted the *in vivo* Matrigel plug assay in male SCID mice. Matrigel mixed with WT hESC-ECs, TKO hESC-ECs, or miR-152 overexpressing hESC-ECs were injected subcutaneously into the flank region of mice. Ten day later, the TKO group showed much lower intensity of red color in Matrigel plugs when compared with that in WT groups, indicating declined angiogenesis level in the TKO group (Figures 6A and 6B). On the contrary, the intensity of red color was obviously increased in Matrigel plug mixed with miR-152 overexpressing hESC-ECs (Figures 6A and 6B). Consistently, the results of H&E staining and immunofluorescence staining for von Willebrand Factor (VWF) also showed a reduction of vascular density in the TKO group and an increase of vascular density in the miR-152 overexpression group, when compared with that in the WT group (Figures 6C and 6D). These data demonstrated the critical role of the miR-148/152 family in maintaining angiogenic capacity of hESC-ECs *in vivo*.

DISCUSSION

Human PSC-derived ECs represent a readily available human cell source for modeling vascular pathology, uncovering novel drug targets, and identifying promising new pharmacotherapies and cell therapies for cardiovascular disease.[3] MiRNAs have emerged as critical modulators of EC differentiation and angiogenesis, and act through dynamically orchestrating various signaling pathways involved in endothelial biology.[27,28] In the present study, we identified the miR-148/152 family as multi-faceted players in endothelial biology. Triple knockout of miR-148/152 family members remarkably reduced the EC differentiation efficiency of hESCs, and inhibited the cell proliferation, migration, and tube formation abilities of hESC-ECs as well. We further demonstrated that MEOX2 is a direct target of the miR-148/152 family in hESC-ECs where silencing of MEOX2 partially restored the miR-148/152 family deletion-caused impairment in angiogenesis.

The miR-148/152 family has been shown to promote cardiomyocyte differentiation from hESCs via synergistic inhibition of DLL1-mediated NOTCH signaling and maintaining the default fate of CHIR-induced cells toward lateral plate mesoderm.[26] Since ECs in our study originated from the same lateral plate mesoderm as cardiomyocytes,[29,30] it is intelligible that the miR-148/152 family could also promote EC differentiation from hESCs. This evidence suggests that the miR-148/152 family may have a universal regulatory effect on cell fate determination into lateral plate mesoderm-derived cells. Consistent with data from cardiomyocyte differentiation, miR-148/152 family deletion led to dramatically increased expression of the NOTCH ligand DLL1 on day 3 of hESC-EC differentiation. Recent study also showed that NOTCH inhibition by DAPT enhanced both the yield and purity of ECs derived from hESCs.[31] Thus, the miR-148/152 family might promote EC differentiation from hESCs through suppressing NOTCH signaling at the stage of lateral plate mesoderm.

There are currently some studies on the regulation of ECs by the miR-148/152 family. For example, miR-152 can alleviate the pathogenesis of atherosclerosis by targeting KLF5 to inhibit inflammation.[32] Previous studies have reported some conflicting evidence concerning the role of miR-148/152 family members in angiogenesis. Consistent with our results in hESC-ECs, Miscianinov et al. demonstrated that miR-148b mimics increased HUVEC proliferation and migration *in vitro*, and promoted wound vascularization *in vivo*.[25] However, Kim et al. showed that the expression of miR-148a and miR-148b was decreased during the differentiation of umbilical cord blood mononuclear cells into outgrowing ECs, and miR-148a/b overexpression significantly reduced migration, filamentous actin remodeling, and angiogenic sprouting in ECs.[24] Here, we demonstrated a pro-angiogenesis effect of the miR-148/152 family in hESC-ECs. To avoid dosage compensation among different members, hESCs with triple deletion of the miR-148/152 family was used in this study. Our data indicated that miR-148/152 family knockout seriously impaired angiogenesis in hESC-ECs via inhibiting three vital events including cell proliferation, migration, and tube formation, while miR-152 overexpression could restore the impaired angiogenesis in miR-148/152 family knockout hESC-ECs.

The currently known signal pathways that regulate the angiogenesis of ECs include PI3K/AKT, NF-κB, VEGF/FLK-1, and SDF1/Cxcr4

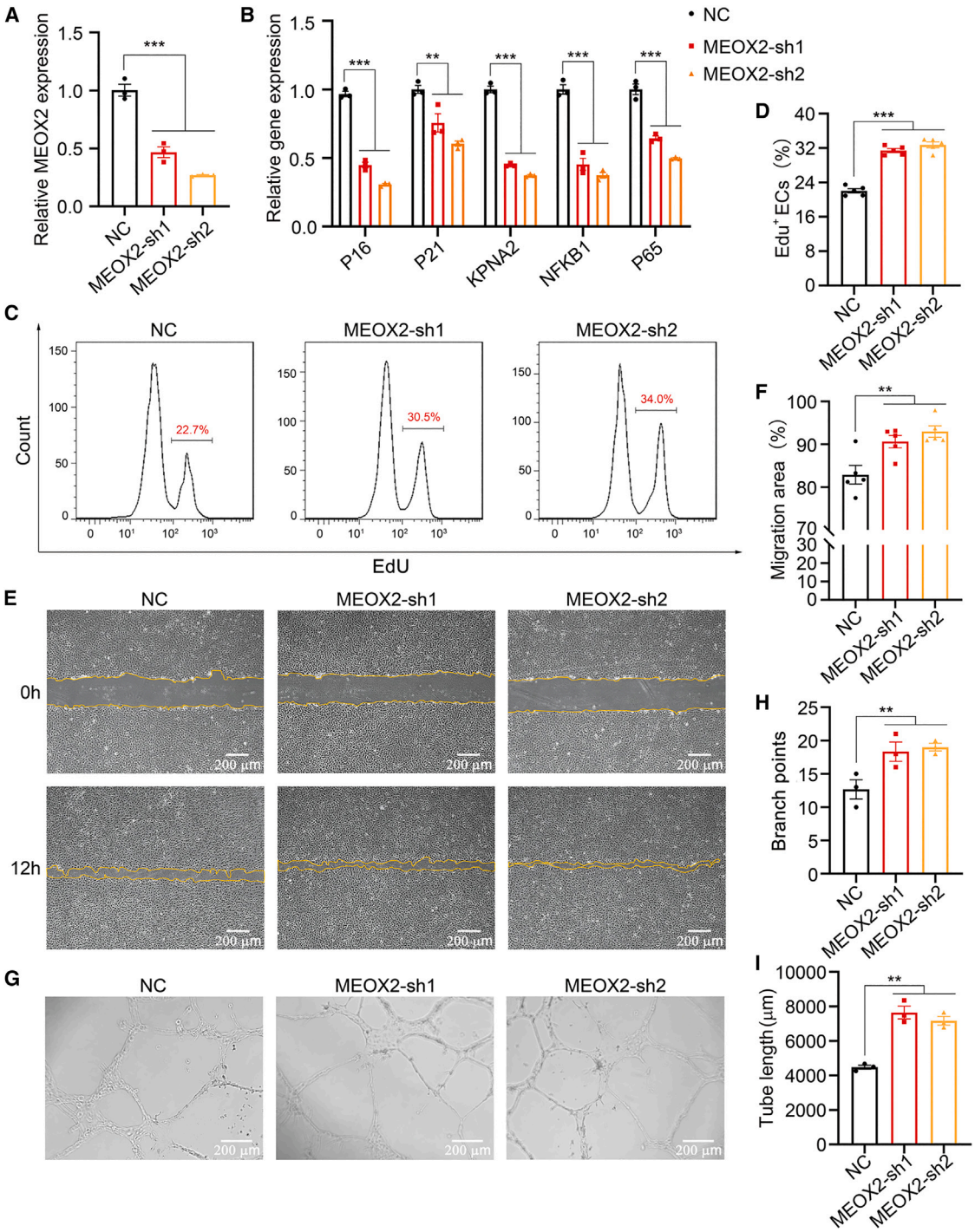

Figure 5. MEOX2 suppression restores the angiogenesis capacity of TKO hESC-derived ECs

(A) Verification of MEOX2 suppression in TKO hESC-derived ECs by RT-qPCR (n = 3 per group). (B) RT-qPCR detection of the downstream genes of MEOX2 in TKO hESC-derived ECs with/without MEOX2 suppression. (C) Flow cytometric assay of EdU incorporation into TKO hESC-derived ECs after transfection with MEOX2 shRNAs. (D) Statistical analysis of EdU-positive ECs in (C) (n = 5 per group). (E) Representative bright-field images of wound-healing assay performed in TKO hESC-derived ECs with/without MEOX2 shRNA transfection. (F) Quantitative statistics of migration area in the wound-healing assays (n = 5 per group). (G) Representative bright-field images of tube formation on Matrigel performed in TKO hESC-derived ECs transfected with/without MEOX2 shRNAs. (H) Statistical analysis of branch points formed in the tube formation assays (n = 3 per group). (I) Statistical analysis of the total length of capillary tubes formed in the tube formation assays (n = 3 per group). Scale bar indicates 200 μm. The data are expressed as the mean ± SEM. **$p < 0.01$, ***$p < 0.001$.

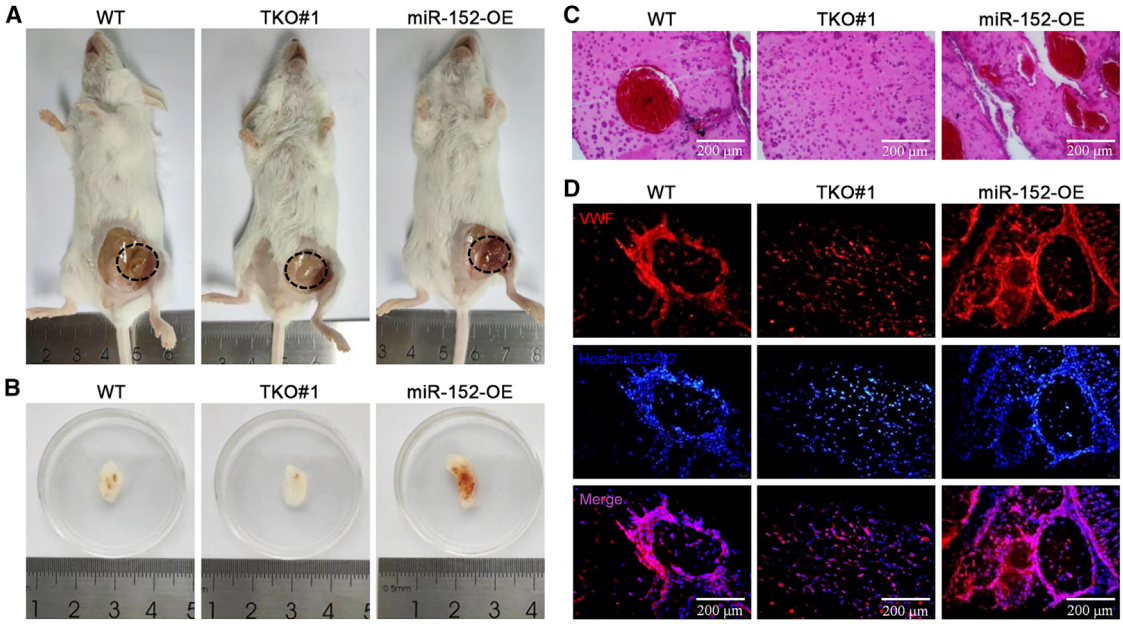

Figure 6. The miR148/152 family regulates angiogenic capacity of hESC-derived ECs *in vivo*

(A) Representative images of *in situ* (highlighted in circle) Matrigel plug at day 10 post injection of Matrigel mixed with WT, TKO, or miR-152-overexpressed hESC-ECs (n = 4). (B) Representative images of Matrigel plugs isolated from mice at day 10 post injection. (C) Representative H&E staining images of the explanted Matrigel plug sections. (D) Representative images of immunofluorescence staining for VWF (red) on the explanted Matrigel plug sections. Nuclei were stained with Hoechst 33342 (blue). Scale bar indicates 200 μm.

pathways.[33,34] In this study, we identified MEOX2 as a direct target of the miR-148/152 family that regulates angiogenesis in hESC-ECs. MEOX2 is a transcription factor that abundantly expresses in resting ECs, inhibits EC activation, and induces cell-cycle arrest.[35] However, the expression of MEOX2 is rapidly down-regulated under the action of serum or pro-angiogenesis and pro-inflammatory factors.[36] Consistently, we observed increased expression of MEOX2, along with impaired angiogenesis, in miR-148/152 family knockout hESC-ECs, while knockdown of MEOX2 led to increase of angiogenesis ability of the TKO hESC-ECs. Thus, we believe that the miR-148/152 family promotes angiogenesis by negative regulation of MEOX2-mediated pathways. Interestingly, miR-148a was recently shown to promote myogenesis via direct targeting of MEOX2 in chicken skeletal muscle satellite cells.[37] These data indicate MEOX2 could mediate multiple functions of the miR-148/152 family in different cells.

Endothelial dysfunction is a leading cause of cardiovascular disease, and hPSC-EC transplantation has shown great promise for therapeutic angiogenesis during tissue repair and regeneration.[38–40] Multiple strategies, including genetic modification and pretreatment with small molecules, have been tested to augment cell survival and function of ECs.[41,42] Our results indicate that the miR-148/152 family can optimize angiogenesis ability of ECs both *in vitro* and *in vivo*. Therefore, we believe that overexpression of the miR-148/152 family or interference with the target gene MEOX2 before cell transplantation may be used as a method to optimize the transplantation of ECs.

In conclusion, our data demonstrate that the miR-148/152 family is crucial for hPSC differentiation into ECs and maintaining the angiogenesis ability of hPSC-ECs, while MEOX2 is a direct target of the miR-148/152 family involved in angiogenesis. The miR-148/152 family might be used as a target to enhance the functional benefit of EC therapy and promote endogenous revascularization.

MATERIALS AND METHODS

Cell culture

The miR-148a/148b/152 triple-knockout hESC lines (TKO#1 and TKO#2) were previously established from the wild-type H1 hESC line (WT) using CRISPR-Cas9-based genome editing.[26] Stem cells were routinely maintained in PSCeasy medium (Cellapy, China) on Matrigel-coated plates (Corning, USA), and were passaged with 0.5 mM EDTA. HUVECs and EA.hy926 cells were cultured in endothelial cell medium (ECM) (ScienCell, USA) in 0.1% gelatin-coated Petri dishes, and passaged with 0.125% trypsin at approximately 70%–80% density. All cell cultures were maintained in a humidified 5% CO_2 incubator at 37°C.

Differentiation of hESCs into ECs

When hESCs reach 90% density, the cell culture medium was changed to the chemically defined differentiation medium CDM3, which consists of RPMI 1640 medium (Thermo Fisher, USA), 500 μg/mL recombinant human albumin (Sigma-Aldrich, USA), and 213 μg/mL L-ascorbic acid 2-phosphate (Sigma-Aldrich, USA). According previous description, the cells were successively treated with 6 μM

CHIR99021 (Sigma-Aldrich, USA) for 2 days (day 0–1), 50 ng/mL bFGF (Novoprotein, USA) for 1 day (day 2), as well as a combination of 50 ng/mL VEGF (Novoprotein, USA) and 25 ng/mL BMP4 (Peprotech, USA) for 3 days (day 3–5).[43] All the hESC-differentiated cells were collected on day 6 for subsequent MACS and flow cytometry analysis.

MACS for CD34$^+$ ECs

After the induction of EC differentiation, cells were dissociated with 0.125% trypsin in 0.2% EDTA. The single-cell suspension was incubated with the anti-CD34 coupled magnetic beads (Miltenyi, Germany), followed by magnetic cell separation to enrich CD34$^+$ ECs as per the manufacturer's instruction. The CD34$^+$ ECs were collected for further experiments.

DiI-ac-LDL uptake assay

Cells were incubated with ECM with 10 μg/mL DiI fluorescent dye-labeled acetylated low-density lipoprotein (DiI-ac-LDL, Biomedical Technologies, USA) at 37°C for 4 h. Cells were then fixed with 4% paraformaldehyde (PFA) in phosphate-buffered saline (PBS), and the nuclei were stained with Hoechst 33342. Photographs were captured under an Olympus LX51 fluorescence microscope (Olympus, Japan).

Tube formation assay *in vitro*

ECs were seeded on a solid layer of growth factor reduced Matrigel (Corning, USA) in a 96-well plate (1×10^4 cells per well), and cultured in ECM. Images were captured under an Olympus LX51 fluorescence microscope (Olympus, Japan) every 2 h for 8–20 h after plating. ImageJ software was used to count the number and length of tubes formed by ECs.

EdU-based flow cytometry assay for cell proliferation

ECs were cultured in the 35-mm cell culture dishes as described above for 3 days, and were then incubated in ECM containing 50 μM EdU at 37°C for 4 h. After digestion with 0.125% trypsin, these cells were fixed with 4% PFA and permeabilized with 0.2% Triton X-100 (Sigma-Aldrich, USA). EdU incorporated into the DNA of proliferating cells was labeled with Alexa Fluor 647 according to the instructions of the BeyoClick EdU Cell Proliferation Kit (Beyotime, China). The rate of EdU-positive cells was analyzed on a Guava easyGyte 8 Flow Cytometer (EMD Millipore, Germany).

Cell counting assay

ECs were digested with 0.125% trypsin in 0.2% EDTA, and were suspended in ECM. Following counting cells with the hemocytometer, the number of total cells was calculated using the following formula: Total number = Average cell number per large square × dilution factor $\times 10^4 \times$ original volume of cell suspension.

Cellular apoptosis assay

Cell apoptosis was induced by exposing ECs to 200 μM of H_2O_2 in fresh medium for 2 h. Cells with/without H_2O_2 treatment were then harvested as single-cell suspension after digestion with 0.125% trypsin. Apoptosis rate was determined by flow cytometry using an Annexin V-APC staining kit (eBioscience, USA) according to the manufacturer's instructions.

Wound-healing assay

Wound-healing assay was used to evaluate the ability of cell migration *in vitro*. ECs were seeded on a 24-well culture plate at a density of 1.5×10^5 cells per well to obtain a confluent cell monolayer. A cell-free area within the confluent monolayer was generated by scratching with a 200-μL pipette tip. The debris was removed by washing cells with Dulbecco's PBS and refreshing the cell culture medium. Cell migration into the wound was monitored and captured for 12 h under an Olympus LX51 fluorescence microscope (Olympus, Japan). Scratch closure was quantified using ImageJ software.

In vivo Matrigel plug assay

According previous study, the Matrigel plug assay was evaluated in male SCID mice aged 8 weeks with the approval of the Laboratory Animal Research Committee of Soochow University.[43] WT, TKO, and miR-152-overexpressing hESC-ECs (0.5×10^7 cells per plug, n = 4 for each group) were resuspended in 400 μL Matrigel, and were then injected subcutaneously into the flank region of mice. All mice were euthanized at day 10 post injection. Matrigel plugs were photographed and subjected to H&E staining and immunostaining of EC markers to evaluated angiogenesis.

RNA isolation and real-time PCR

Total RNAs, which include mRNAs and miRNAs, were extracted from cells using TRIzol Reagent (Sigma-Aldrich, USA) according to the manufacturer's manual. Takara PrimeScript RT Reagent kit (Takara, Japan) was used to synthesize cDNAs from total RNAs. For miRNA detection, the specific stem-loop primers for each miRNA were utilized in a cDNA synthesis reaction.[26] Real-time PCR (qPCR) was performed on an Applied Biosystems StepOnePlus Real-Time PCR System (Thermo Fisher, USA). The qPCR primer sequences are listed in Table S1. The 18S RNA was used as the internal reference gene.

Immunofluorescence staining

Cells or frozen sections were fixed with 4% PFA for 15 min, followed by permeabilization with 0.2% Triton X-100 (Sigma-Aldrich, USA) for 5 min. After washing with PBS, cells or sections were incubated successively with 5% BSA in PBS for 1 h at room temperature and the indicated primary antibodies overnight at 4°C. Subsequently, cells or sections were washed with PBST (0.1% Tween 20 in PBS), and incubated in darkness with the corresponding fluorescent secondary antibody at room temperature for 1 h. Hoechst 33342 was used for the nuclear staining. Images were captured with an LSM880 Zeiss confocal laser scanning microscope (Carl Zeiss, Germany) and were further analyzed using ImageJ software. Antibodies for immunofluorescence staining are listed in Table S2.

Dual luciferase assay

To construct the luciferase reporter vectors, the human MEOX2 3′-UTR fragments containing the potential binding sites of

miR-148/152 family members were amplified by PCR using KOD-Plus-Neo DNA polymerase (Toyobo, Japan), and were inserted into the KpnI/XhoI locus of the PGL3 control vectors (Promega, USA) downstream of the firefly luciferase gene. The target-site mutant MEOX2 3′-UTR vectors were generated by replacing the target sequences "UGCACUGA" with "UACUACAC." The WT or mutated MEOX2 3′-UTR reporter vectors were transfected into HEK293T cells, along with miR-152 mimics (Ribobio, China) using a Lipofectamine 2000 Transfection Reagent (Thermo Fisher, USA). The Renilla luciferase reporter vectors (pRL-TK, Promega, USA) were used as an internal reference for transfection efficiency. The cells were lysed 48 h after transfection, and luciferase activity was analyzed using the dual luciferase reporter assay system (Promega, USA) according to the manufacturer's instructions.

Lentiviral overexpression of miR-152

To generate the lentiviral vector overexpressing human miR-152 (pLV-miR-152-OE), DNA fragments covering miR-152 pre-miRNA and its flank regions (∼200 nucleotides each side) were amplified by PCR using KOD-Plus-Neo DNA polymerase (Toyobo, Japan), and were cloned into the MluI/ClaI sites of the pLVTHM vector (Addgene, USA). The pLVTHM or pLV-miR-152-OE vectors were then transfected into HEK293T cells together with the packed plasmid psPAX2 and pMD2.G. The control and miR-152-overexpressing lentiviral particles in culture medium were concentrated with PEG 8000 (Sigma-Aldrich, USA), and further used to infect WT and TKO ECs at the same multiplicity of infection.

Lentiviral shRNA knockdown of MEOX2

In this experiment, MEOX2 interference was mainly achieved through lentivirus-mediated shRNA transfection. The shRNA sequences targeting MEOX2 were designed by BLOCK-iT RNAi Designer (Thermo Fisher, USA) and synthesized by Suzhou Jinweizhi Biotechnology Co., Ltd (China). The shRNA fragments were cloned into the MluI/ClaI sites of the pLVTHM vector (Addgene, USA). The new developed vectors were then transfected into HEK293T cells together with the helper plasmids psPAX2 and pMD2.G for virus packaging, as mentioned above.

Statistical analysis

All experimental analyses were performed at least three times. The data were analyzed using GraphPad Prism version 8.0, and were expressed as mean ± SEM. Student's t test was used for comparison between two groups. Multiple comparisons were performed using one-way analysis of variance followed by the Bonferroni *post hoc* test. p values <0.05 was considered statistically significant.

DATA AVAILABILITY

The data supporting the findings of this study are available within the article and its supplementary materials.

SUPPLEMENTAL INFORMATION

Supplemental information can be found online at https://doi.org/10.1016/j.omtn.2023.04.020.

ACKNOWLEDGMENTS

This work was funded by the National Key R&D Program of China (2022YFA1104300, 2021YFA1101902), the National Natural Science Foundation of China (81970223, 82241202, 82170364, 82003756), the Natural Science Foundation of Jiangsu Province (BK20201409, BK20200880), and Jiangsu Cardiovascular Medicine Innovation Center (CXZX202210).

AUTHOR CONTRIBUTIONS

W.L., S.H., and M.Y. supervised the entire project. F.D., H.W., and X.H. performed most of the experiments, and analyzed the data. X.J., Y.X., and Y.T. performed endothelial cell differentiation and cell culture. W.L., S.H., and F.D. wrote and revised the manuscript.

DECLARATION OF INTERESTS

The authors declare no competing interests.

REFERENCES

1. Shao, Y., Saredy, J., Yang, W.Y., Sun, Y., Lu, Y., Saaoud, F., Drummer, C., 4th, Johnson, C., Xu, K., Jiang, X., et al. (2020). Vascular endothelial cells and innate immunity. Arterioscler. Thromb. Vasc. Biol. *40*, e138–e152.
2. Marziano, C., Genet, G., and Hirschi, K.K. (2021). Vascular endothelial cell specification in health and disease. Angiogenesis *24*, 213–236.
3. Williams, I.M., and Wu, J.C. (2019). Generation of endothelial cells from human pluripotent stem cells. Arterioscler. Thromb. Vasc. Biol. *39*, 1317–1329.
4. Lin, Y., Gil, C.H., and Yoder, M.C. (2017). Differentiation, evaluation, and application of human induced pluripotent stem cell-derived endothelial cells. Arterioscler. Thromb. Vasc. Biol. *37*, 2014–2025.
5. Ang, L.T., Nguyen, A.T., Liu, K.J., Chen, A., Xiong, X., Curtis, M., Martin, R.M., Raftry, B.C., Ng, C.Y., Vogel, U., et al. (2022). Generating human artery and vein cells from pluripotent stem cells highlights the arterial tropism of Nipah and Hendra viruses. Cell *185*, 2523–2541.e30.
6. Cho, H., Macklin, B.L., Lin, Y.Y., Zhou, L., Lai, M.J., Lee, G., Gerecht, S., and Duh, E.J. (2020). iPSC-derived endothelial cell response to hypoxia via SDF1a/CXCR4 axis facilitates incorporation to revascularize ischemic retina. JCI Insight *5*, e131828.
7. MacAskill, M.G., Saif, J., Condie, A., Jansen, M.A., MacGillivray, T.J., Tavares, A.A.S., Fleisinger, L., Spencer, H.L., Besnier, M., Martin, E., et al. (2018). Robust revascularization in models of limb ischemia using a clinically translatable human stem cell-derived endothelial cell Product. Mol. Ther. *26*, 1669–1684.
8. Ye, L., Chang, Y.H., Xiong, Q., Zhang, P., Zhang, L., Somasundaram, P., Lepley, M., Swingen, C., Su, L., Wendel, J.S., et al. (2014). Cardiac repair in a porcine model of acute myocardial infarction with human induced pluripotent stem cell-derived cardiovascular cells. Cell Stem Cell *15*, 750–761.
9. Gu, M., Nguyen, P.K., Lee, A.S., Xu, D., Hu, S., Plews, J.R., Han, L., Huber, B.C., Lee, W.H., Gong, Y., et al. (2012). Microfluidic single-cell analysis shows that porcine induced pluripotent stem cell-derived endothelial cells improve myocardial function by paracrine activation. Circ. Res. *111*, 882–893.
10. Ambros, V. (2004). The functions of animal microRNAs. nature *431*, 350–355.
11. Conrad, P., Hodgkinson, M.H.K., dal-Pra, S., maria, M., and victor, J.D. (2015). MicroRNAs and cardiac regeneration. Circ. Res. *116*, 715–736.
12. Njock, M.S., and Fish, J.E. (2017). Endothelial miRNAs as cellular messengers in cardiometabolic diseases. Trends Endocrinol. Metab. *28*, 237–246.
13. Schober, A., Nazari-Jahantigh, M., Wei, Y., Bidzhekov, K., Gremse, F., Grommes, J., Megens, R.T.A., Heyll, K., Noels, H., Hristov, M., et al. (2014). MicroRNA-126-5p promotes endothelial proliferation and limits atherosclerosis by suppressing Dlk1. Nat. Med. *20*, 368–376.
14. Liu, X.L., Wang, G., Song, W., Yang, W.X., Hua, J., and Lyu, L. (2018). microRNA-137 promotes endothelial progenitor cell proliferation and angiogenesis in cerebral

ischemic stroke mice by targeting NR4A2 through the Notch pathway. J. Cell. Physiol. *233*, 5255–5266.

15. Fang, Y., Shi, C., Manduchi, E., Civelek, M., and Davies, P.F. (2010). MicroRNA-10a regulation of proinflammatory phenotype in athero-susceptible endothelium in vivo and in vitro. Proc. Natl. Acad. Sci. USA *107*, 13450–13455.

16. Chiba, T., Cerqueira, D.M., Li, Y., Bodnar, A.J., Mukherjee, E., Pfister, K., Phua, Y.L., Shaikh, K., Sanders, B.T., Hemker, S.L., et al. (2021). Endothelial-derived miR-17 approximately 92 promotes angiogenesis to Protect against renal ischemia-reperfusion injury. J. Am. Soc. Nephrol. *32*, 553–562.

17. Kane, N.M., Howard, L., Descamps, B., Meloni, M., McClure, J., Lu, R., McCahill, A., Breen, C., Mackenzie, R.M., Delles, C., et al. (2012). Role of microRNAs 99b, 181a, and 181b in the differentiation of human embryonic stem cells to vascular endothelial cells. Stem Cell. *30*, 643–654.

18. Luo, Z., Wen, G., Wang, G., Pu, X., Ye, S., Xu, Q., Wang, W., and Xiao, Q. (2013). MicroRNA-200C and -150 play an important role in endothelial cell differentiation and vasculogenesis by targeting transcription repressor ZEB1. Stem Cell. *31*, 1749–1762.

19. Di Bernardini, E., Campagnolo, P., Margariti, A., Zampetaki, A., Karamariti, E., Hu, Y., and Xu, Q. (2014). Endothelial lineage differentiation from induced pluripotent stem cells is regulated by microRNA-21 and transforming growth factor β2 (TGF-β2) pathways. J. Biol. Chem. *289*, 3383–3393.

20. Fish, J.E., Santoro, M.M., Morton, S.U., Yu, S., Yeh, R.F., Wythe, J.D., Ivey, K.N., Bruneau, B.G., Stainier, D.Y.R., and Srivastava, D. (2008). miR-126 regulates angiogenic signaling and vascular integrity. Dev. Cell *15*, 272–284.

21. Friedrich, M., Pracht, K., Mashreghi, M.F., Jäck, H.M., Radbruch, A., and Seliger, B. (2017). The role of the miR-148/-152 family in physiology and disease. Eur. J. Immunol. *47*, 2026–2038.

22. Xu, Q., Jiang, Y., Yin, Y., Li, Q., He, J., Jing, Y., Qi, Y.T., Xu, Q., Li, W., Lu, B., et al. (2013). A regulatory circuit of miR-148a/152 and DNMT1 in modulating cell transformation and tumor angiogenesis through IGF-IR and IRS1. J. Mol. Cell Biol. *5*, 3–13.

23. Raso, A., Dirkx, E., Philippen, L.E., Fernandez-Celis, A., De Majo, F., Sampaio-Pinto, V., Sansonetti, M., Juni, R., El Azzouzi, H., Calore, M., et al. (2019). Therapeutic delivery of miR-148a suppresses ventricular dilation in heart failure. Mol. Ther. *27*, 584–599.

24. Kim, H., Ko, Y., Park, H., Zhang, H., Jeong, Y., Kim, Y., Noh, M., Park, S., Kim, Y.M., and Kwon, Y.G. (2019). MicroRNA-148a/b-3p regulates angiogenesis by targeting neuropilin-1 in endothelial cells. Exp. Mol. Med. *51*, 1–11.

25. Miscianinov, V., Martello, A., Rose, L., Parish, E., Cathcart, B., Mitić, T., Gray, G.A., Meloni, M., Al Haj Zen, A., and Caporali, A. (2018). MicroRNA-148b targets the TGF-β pathway to regulate angiogenesis and endothelial-to-mesenchymal transition during skin wound healing. Mol. Ther. *26*, 1996–2007.

26. Fang, X., Miao, S., Yu, Y., Ding, F., Han, X., Wu, H., Zhao, Z.A., Wang, Y., Hu, S., and Lei, W. (2019). MIR148A family regulates cardiomyocyte differentiation of human embryonic stem cells by inhibiting the DLL1-mediated NOTCH signaling pathway. J. Mol. Cell. Cardiol. *134*, 1–12.

27. Harding, A., Cortez-Toledo, E., Magner, N.L., Beegle, J.R., Coleal-Bergum, D.P., Hao, D., Wang, A., Nolta, J.A., and Zhou, P. (2017). Highly efficient differentiation of endothelial cells from pluripotent stem cells requires the MAPK and the PI3K pathways. Stem Cell. *35*, 909–919.

28. Kir, D., Schnettler, E., Modi, S., and Ramakrishnan, S. (2018). Regulation of angiogenesis by microRNAs in cardiovascular diseases. Angiogenesis *21*, 699–710.

29. Loh, K.M., Chen, A., Koh, P.W., Deng, T.Z., Sinha, R., Tsai, J.M., Barkal, A.A., Shen, K.Y., Jain, R., Morganti, R.M., et al. (2016). Mapping the Pairwise choices leading from pluripotency to human bone, heart, and other mesoderm cell types. Cell *166*, 451–467.

30. Nguyen, J., Lin, Y.Y., and Gerecht, S. (2021). The next generation of endothelial differentiation: tissue-specific ECs. Cell Stem Cell *28*, 1188–1204.

31. Reichman, D., Man, L., Park, L., Lis, R., Gerhardt, J., Rosenwaks, Z., and James, D. (2016). Notch hyper-activation drives trans-differentiation of hESC-derived endothelium. Stem Cell Res. *17*, 391–400.

32. Wang, W., Zhang, Y., Wang, L., Li, J., Li, Y., Yang, X., and Wu, Y. (2019). mircroRNA-152 prevents the malignant progression of atherosclerosis via down-regulation of KLF5. Biomed. Pharmacother. *109*, 2409–2414.

33. Semo, J., Sharir, R., Afek, A., Avivi, C., Barshack, I., Maysel-Auslender, S., Krelin, Y., Kain, D., Entin-Meer, M., Keren, G., and George, J. (2014). The 106b∼25 microRNA cluster is essential for neovascularization after hindlimb ischaemia in mice. Eur. Heart J. *35*, 3212–3223.

34. Hasegawa, Y., Saito, T., Ogihara, T., Ishigaki, Y., Yamada, T., Imai, J., Uno, K., Gao, J., Kaneko, K., Shimosawa, T., et al. (2012). Blockade of the nuclear factor-κB pathway in the endothelium prevents insulin resistance and prolongs life spans. Circulation *125*, 1122–1133.

35. Chen, Y., Rabson, A.B., and Gorski, D.H. (2010). MEOX2 regulates nuclear factor-kappaB activity in vascular endothelial cells through interactions with p65 and IkappaBbeta. Cardiovasc. Res. *87*, 723–731.

36. Wu, Z., Guo, H., Chow, N., Sallstrom, J., Bell, R.D., Deane, R., Brooks, A.I., Kanagala, S., Rubio, A., Sagare, A., et al. (2005). Role of the MEOX2 homeobox gene in neurovascular dysfunction in Alzheimer disease. Nat. Med. *11*, 959–965.

37. Yin, H., He, H., Cao, X., Shen, X., Han, S., Cui, C., Zhao, J., Wei, Y., Chen, Y., Xia, L., et al. (2020). MiR-148a-3p regulates skeletal muscle satellite cell differentiation and apoptosis via the PI3K/AKT signaling pathway by targeting Meox2. Front. Genet. *11*, 512.

38. Cooke, J.P., and Losordo, D.W. (2015). Modulating the vascular response to limb ischemia: angiogenic and cell therapies. Circ. Res. *116*, 1561–1578.

39. Veith, A.P., Henderson, K., Spencer, A., Sligar, A.D., and Baker, A.B. (2019). Therapeutic strategies for enhancing angiogenesis in wound healing. Adv. Drug Deliv. Rev. *146*, 97–125.

40. Hu, S., Zhao, M.T., Jahanbani, F., Shao, N.Y., Lee, W.H., Chen, H., Snyder, M.P., and Wu, J.C. (2016). Effects of cellular origin on differentiation of human induced pluripotent stem cell-derived endothelial cells. JCI Insight *1*, e85558.

41. Bardita, C., Predescu, D., Justice, M.J., Petrache, I., and Predescu, S. (2013). In vivo knockdown of intersectin-1s alters endothelial cell phenotype and causes microvascular remodeling in the mouse lungs. Apoptosis *18*, 57–76.

42. Luo, Y., Xu, Z., Wan, T., He, Y., Jones, D., Zhang, H., and Min, W. (2010). Endothelial-specific transgenesis of TNFR2 promotes adaptive arteriogenesis and angiogenesis. Arterioscler. Thromb. Vasc. Biol. *30*, 1307–1314.

43. Yang, Z., Yu, M., Li, X., Tu, Y., Wang, C., Lei, W., Song, M., Wang, Y., Huang, Y., Ding, F., et al. (2022). Retinoic acid inhibits the angiogenesis of human embryonic stem cell-derived endothelial cells by activating FBP1-mediated gluconeogenesis. Stem Cell Res. Ther. *13*, 239.